Inflammation, Vol. 44, No. 2, April 2021 (© 2020)
DOI: 10.1007/s10753-020-01370-2

ORIGINAL ARTICLE

Isoliquiritigenin Reduces LPS-Induced Inflammation by Preventing Mitochondrial Fission in BV-2 Microglial Cells

Dong Gil Lee,[1] Bo Ra Nam,[1] Jae-Won Huh,[2] and Dong-Seok Lee[1,3]

Received 17 April 2020; accepted 19 October 2020

Abstract— Excessive microglial cell activation in the brain can lead to the production of various neurotoxic factors (*e.g.*, pro-inflammatory cytokines, nitric oxide) which can, in turn, initiate neurodegenerative processes. Recent research has been reported that mitochondrial dynamics regulate the inflammatory response of lipopolysaccharide (LPS). Isoliquiritigenin (ISL) is a compound found in *Glycyrrhizae radix* with anti-inflammatory and antioxidant properties. In this study, we investigated the function of ISL on the LPS-induced pro-inflammatory response in BV-2 microglial cells. We showed that ISL reduced the LPS-induced increase in pro-inflammatory mediators (*e.g.*, nitric oxide and pro-inflammatory cytokines) *via* the inhibition of ERK/p38/NF-κB activation and the generation of reactive oxygen species (ROS). Furthermore, ISL inhibited the excessive mitochondrial fission induced by LPS, regulating mitochondrial ROS generation and pro-inflammatory response by suppressing the calcium/calcineurin pathway to dephosphorylate Drp1 at the serine 637 residue. Interestingly, the ISL pretreatment reduced the number of apoptotic cells and levels of cleaved caspase3/PARP, compared to LPS-treated cells. Our findings suggested that ISL ameliorated the pro-inflammatory response of microglia by inhibiting dephosphorylation of Drp1 (Ser637)-dependent mitochondrial fission. This study provides the first evidence for the effects of ISL against LPS-induced inflammatory response related and its link to mitochondrial fission and the calcium/calcineurin pathway. Consequently, we also identified the protective effects of ISL against LPS-induced microglial apoptosis, highlighting the pharmacological role of ISL in microglial inflammation-mediated neurodegeneration.

Dong Gil Lee and Bo Ra Nam contributed equally to this work.

Supplementary Information The online version contains supplementary material available at https://doi.org/10.1007/s10753-020-01370-2.

[1] School of Life Sciences, BK21 Plus KNU Creative BioResearch Group, Kyungpook National University, Daegu, Republic of Korea
[2] National Primate Research Center, Korea Research Institute of Bioscience and Biotechnology (KRIBB), Cheongju, Chungcheongbuk-do, Republic of Korea
[3] To whom correspondence should be addressed at School of Life Sciences, BK21 Plus KNU Creative BioResearch Group, Kyungpook National University, Daegu, Republic of Korea. E-mail: lee1@knu.ac.kr

KEY WORDS: microglia; lipopolysaccharide; isoliquiritigenin; mitochondrial fission; oxidative stress; calcium.

INTRODUCTION

Microglia are immune cells found in the human brain, which play an important role in the CNS given their role in neuroprotection [1, 2]. Microglia normally help neurons function and monitor the neuronal homeostasis; however, excessive microglial activity (*e.g.*, caused by neuroinflammation, nerve damage, or neurodegeneration) can lead to apoptosis in neurons [3]. Activated microglia induced an inflammatory response, such as nitric oxide production, tumor necrosis factor-alpha, or NF-kB-mediated pathways [3]. Given the prominence of excessive microglial activity in several degenerative diseases [4, 5], it is essential to understand the specific mechanisms of pro-inflammatory response by activated microglia.

Isoliquiritigenin (ISL), isolated from *Glycyrrhizae radix*, is known to have an antimicrobial, anti-inflammatory, and antiviral properties [6, 7]. ISL has been found to induce apoptosis in tumor cells [8], inhibit the NF-kB-mediated inflammatory response, and downregulate mitogen-activated protein kinase (MAPK) using lipopolysaccharides (LPS) in raw 264.7 cells, a macrophage [9]. Additionally, ISL mitigates inflammatory response through the Nrf2 and NF-kB pathways [6]. Based on the above facts, we hypothesized that ISL could mitigate the LPS-induced inflammatory response in microglia and investigated the specific mechanism of protective effects against inflammation.

Many neurological disorders are closely associated with the regulation of reactive oxygen species (ROS) and mitochondrial dynamics [10, 11]. ROS participate in various cellular functions (*e.g.*, acting as secondary messengers), but excessive ROS can damage DNA, proteins, and lipids intracellularly, consequently causing cellular dysfunction [12, 13]. Furthermore, ROS are known to cause an inflammatory response in microglia [14]. LPS-induced ROS production activates MAPK (*e.g.*, ERK, JNK, and p-38), and NF-kB mediates inflammation signaling [15]. Several studies have shown that mitochondrial ROS plays an important role in innate immunity through the activation of MAPK [16, 17]. Dysregulation of mitochondrial functions has been reported in many neurological disorders, such as Alzheimer's and Parkinson's disease [18, 19]. The balance of mitochondrial dynamics (*e.g.*, fission and fusion) plays an important role in cell function [19, 20]. Mitochondrial fission is regulated by dynamin-related protein 1 (Drp1) and mitochondrial fission 1 (Fis1), while fusion is regulated by mitofusin 1 (Mfn1), mitofusin 2 (Mfn2), and optic atrophy 1 (Opa1) [18, 19]. In a previous study, LPS-induced mitochondrial fission was achieved *via* the dephosphorylation of Drp1 at serine 637 residue in microglia [21]. The dephosphorylation of Drp1 serine 637 is regulated by calcineurin, a serine/threonine phosphatase. Calcineurin is activated by calcium/calmodulin-dependent or calmodulin-independent (calcium/calpain) pathways [22]. Because ISL has been reported to have protective effect against mitochondrial dysfunction through its antioxidant properties [23, 24], we hypothesized that antioxidant-ISL has a protective effect against LPS-induced mitochondrial fission and inflammatory response.

Based on the above research, this study aims to investigate the effect of ISL against LPS-induced inflammatory response and how this relates to mitochondrial dynamics and signaling pathways. It also aims to establish the precise mechanism of protective effects in BV-2 microglial cells. The results will clarify whether ISL is suitable candidate for drug therapy in inflammatory-mediated neurological disorders.

MATERIAL AND METHODS

Chemicals and Reagents

Lipopolysaccharides from *Escherichia coli* serotype O26:B6 and isoliquiritigenin (ISL) were obtained from Sigma-Aldrich (St. Louis, MO, USA).

Cell Culture and Treatment

BV-2 murine microglial cells were immortalized by infection with v-raf/c-myc recombination retrovirus (Blasi et al., 1990), provided by Dr. Jau-Shyong Hong of the National Institute of Environmental Health Sciences (NC, USA). BV-2 cells were reproduced in Dulbecco's Modified Eagle's Medium (Welgene, Daegu, Korea), containing 10% fetal bovine serum (Thermo Fisher Scientific, Waltham, MA, USA) and 1% penicillin/streptomycin (Welgene). Cells were maintained at 37 °C in a humidified 5% CO_2 incubator (SANYO, Osaka, Japan) then subcultured at a density of 2×10^5 cells in 60 Φ plates and left to grow for 24 h before the experiments started. Exponentially growing BV-2 cells were pretreated with ISL for 1 h, followed by stimulation with 1 μg/mL LPS.

Plasmid Construction and Stably DsRed2-Mito Transduced BV-2 Cells

The DsRed2-mito gene was obtained from pDsRed2-mito (Clontech, Mountain View, CA, USA). The coding nucleotide sequences for DsRed2-mito were amplified by PCR using LA Taq polymerase (Takara, Shiga, Japan). This gene was cloned into pCR8/GW/TOPO (Invitrogen, Carlsbad, CA, USA) and inserted into pLenti6.3/V5-DEST (Invitrogen) using LR Clonase (Invitrogen). Constructed vectors were confirmed by restriction mapping and DNA sequencing. Approximately 1×10^5 BV-2 cells were seeded into 6-well plates and grown for 24 h before transfection. Then, 1 μg of pLenti6.3-DsRed2-mito plasmid was transfected into BV-2 cells using Effectene (QIAGEN, Valencia, CA, USA), according to the manufacturer's instructions. One day after transfection, DsRed2-mito transfected BV-2 cells were selected using 8 μg/mL blasticidin (Invitrogen).

RNA Isolation and RT-PCR

Total RNA was isolated from BV-2 cells using the TRI-Solution (BioScience Technology, Seoul, Korea), according to the manufacturer's instructions. cDNA was synthesized from 1 μg total RNA using a Reverse Transcription (RT) Premix (Bioneer, Daejeon, Korea). PCR was performed using gene-specific primers and the PCR premix (Bioneer). The following PCR primers were used: TNF-α forward (5′- AGTTCTATGGCCCAGACCCT -3′), TNF-α reverse (5′- GTGGGTGAGGAGCACGTAGT -3′), IL-1β forward (5′- CGACAAAAACCTGTGGCCT -3′), IL-1β reverse (5′- AGGCCACAGGTATTTTGTCG -3′), IL-6 forward (5′- AGTTGCCTTCTTGGGACTGA -3′), IL-6 reverse (5′- TTCTGCAAGTGCATCATCGT -3′), GAPDH forward (5′- ACCACAGTCCATGC CATCAC -3′), GAPDH reverse (5′- TCCACCAC CCTGTTGCTGTA -3′).

Western Blot Analysis

Whole protein lysates were prepared using a PRO-PREP protein extraction solution (Intron Biotechnology, Korea). Protein quantification was performed using an Infinite F50 microplate reader (TECAN, Männedorf, Switzerland). Equal amounts of protein were separated by electrophoresis on 10–12% sodium dodecyl sulfate (SDS)-polyacrylamide gel. The separated proteins were then transferred onto nitrocellulose membranes (Pall Corporation, NY, USA). Membranes were blocked with 5% skimmed milk (BD Biosciences, New Jersey, USA) and membranes were incubated overnight at 4 °C with the following primary antibodies: anti-ERK, anti-phosphorylated (p)-ERK, anti-JNK, anti-p-JNK, anti-p38, anti-p-p38, anti-p-IκB, anti-p-Drp1 (Ser616), anti-p-Drp1 (Ser637) anti-cleaved caspase-3, and anti-PARP (Cell Signaling, MA, USA); anti-iNOS (Abcam, MA, USA); anti-Cox-2, anti-β-actin, anti-IκB, anti-Drp1, anti-Bcl-2, and anti-Bax (Santa Cruz, TX, USA); and NF-κB(Ab Frontier, Korea). Membranes were washed six times with 10 mM Tris–HCl (pH 7.5) containing 150 mM NaCl and 0.1% Tween 20 (TBST) and then subsequently incubated with horseradish peroxidase-conjugated goat anti-rabbit and anti-mouse antibodies (Thermo Fisher Scientific) before being incubated overnight at 4 °C. After removing excess secondary antibodies, membranes were washed six times with TBST. Specific binding was detected using Clarity Western ECL Substrate (Bio-Rad, CA, USA), according to the manufacturer's instructions.

Cell Viability (CCK) Assay

BV-2 cells were cultured 1×10^5 cells in 6-well plates, and then different concentrations of ISL were added to the wells. After 24 h, cells were treated with 50 μL CCK for each well and incubated for 1 h at 37 °C. Absorbance was then measured at 450 nm using an Infinite F50 microplate reader (TECAN, Switzerland).

Flow Cytometry

BV2 cells (2×10^5) were cultured in 60 Φ plates for 24 h. Cells were then incubated with or without ISL for 30 min before LPS treatment, which lasted 24 h. Next, cells were harvested by trypsinization. To measure intracellular mitochondrial ROS and calcium levels, harvested cells were washed with PBS, then incubated with 2.5 μM of CM-H2DCFDA, MitoSOX, and Fluo-4 AM (Thermo Fisher Scientific) for 15 min at 37 °C. Finally, cells were washed twice with PBS and analyzed by flow cytometry (FACSverse; BD Biosciences).

NO Detection

The amount of NO was measured in the cell-free culture supernatant using a commercially available NO detection kit (Intron Biotechnology), according to the manufacturer's instructions. Content absorbance was measured at 450 nm.

Mitochondria Imaging and Analysis

DsRed2-mito expressing BV-2 cells were seeded on 0.1% poly-D-lysine-coated round coverslips (diameter, 24 mm; Marienfeld, Lauda-Königshofen, Germany). The cells were then pretreated with or without ISL (10 μM) for 30 min before treatment with 1 μg/mL LPS for 24 h. The BV-2 cells were washed twice with PBS and then fixed with 4% paraformaldehyde (Sigma) in PBS for 1 h. After washing twice with PBS, coverslips were mounted on slides using VECTASHIELD mounting medium (VECTOR Laboratories, CA, USA). Images were obtained using an LSM-710 confocal microscope (Carl Zeiss, Oberkochen, Germany) with a plan apochromatic 100×/1.40 oil DIC M27 objective lens. Images were processed using a Zeiss LSM image examiner, ZEN 2009 Light Edition (Carl Zeiss). Mitochondrial length was measured using the ImageJ software (NIH, Bethesda, MD, USA), computed from more than 50 mitochondrial particles per cell in a sample of 20 cells.

Intracellular Calcium

The level of intracellular Ca^{2+} was determined using Fluo-4 AM (Invitrogen), a Ca^{2+}-sensitive fluorescent indicator. BV-2 cells were incubated with 5 μM Fluo-4 AM at 37 °C for 30 min. After washing with PBS, the images were observed using a DE/DMI 3000B microscope (Leica, Wetzlar, Germany). Quantification of Ca2+ was performed using the ImageJ software (NIH).

Calpain and Calcineurin Activity

BV-2 cells were seeded at 2×10^5 cells in 60 Φ plates and were grown for 24 h before starting the experiments. Cells were pretreated with or without ISL for 30 min before treatment of LPS for 24 h. Next, whole protein lysates were prepared using an ice-cold NP-40 cell lysis buffer (Thermo Fisher Scientific). Calpain and calcineurin activity was measured using a Calpain-Glo™ Protease Assay (Promega Corporation, Madison, USA) and a Calcineurin Phosphatase Activity Assay Kit (Abcam), respectively, according to the manufacturer's instructions.

Statistical Analysis

Statistical analysis was conducted using the Prism software (GraphPad Prism version 5.0; La Jolla, CA, USA). Data are shown as mean ± standard deviation (SD), as the average of at least three independent experiments ($n \geq 3$). For group comparisons, one-way analysis of variance and Dunnett's multiple comparison tests were performed. Statistical significance was set at $p < 0.05$. Significance is indicated on graphs by an asterisk, whereas p values < 0.01 and < 0.001 are indicated by two and three asterisks, respectively.

RESULTS

ISL Attenuated LPS-Induced Pro-inflammatory Response, Activation of NF-κB, and Phosphorylation of ERK, p38, but Not JNK in BV-2 Microglial Cells

The cytotoxicity of ISL was assessed in dose-dependent (1–20 μM) exposure to BV-2 cells using a CCK assay before investigating the effect of ISL. The result showed that cell viability of BV-2 cells was not affected by ISL at concentrations lower than 10 μM, but was significantly lower at 20 μM ISL (Fig. 1a). Based on this result, we used 10 μM ISL in the following experiments. As high levels of NO production *via* iNOS are known to have toxic effects on the brain, and Cox-2 induces secondary damage to neurons in activated microglia [25, 26], we examined the effect of ISL on LPS-induced microglial activation by measuring NO production and expression of iNOS and Cox-2. Results show that increased LPS-induced NO production was reduced by ISL pretreatment (Fig. 1b) and ISL ameliorated LPS-induced iNOS and Cox-2 expression in BV-2 cells (Fig. 1c). Some studies suggest that NF-κB and MAPK (*e.g.*, ERK, JNK, and p38) are important transcription factors for various pro-inflammatory mediators in activated microglia [27, 28]. Thus, to confirm the effects of ISL on MAPK regulation and NF-κB pathways in LPS-induced BV-2 cells, we assessed the expression levels of phosphorylated IκB, p65 NF-κB, and activation of MAPK. Results show that ISL reduced LPS-induced phosphorylation of IκB and levels of p65 NF-κB, as well as MAPK activation and the consequent phosphorylation of ERK, p38, and JNK (Fig. 1d and e). We also found that LPS-induced increase in mRNA levels of IL-1β, TNF-α, and iNOS were decreased by ISL (Fig. 1f), suggesting that ISL inhibited pro-inflammatory response through regulation of the NF-κB and MAPK pathways in LPS-stimulated BV-2 microglial cells.

ISL Prevents LPS-Induced Mitochondrial Fission *via* Dephosphorylation of Drp1 at Ser637 by Inhibiting ROS Production

Mitochondrial dynamics are known to mediate an inflammatory response in activated microglia [21]. Several

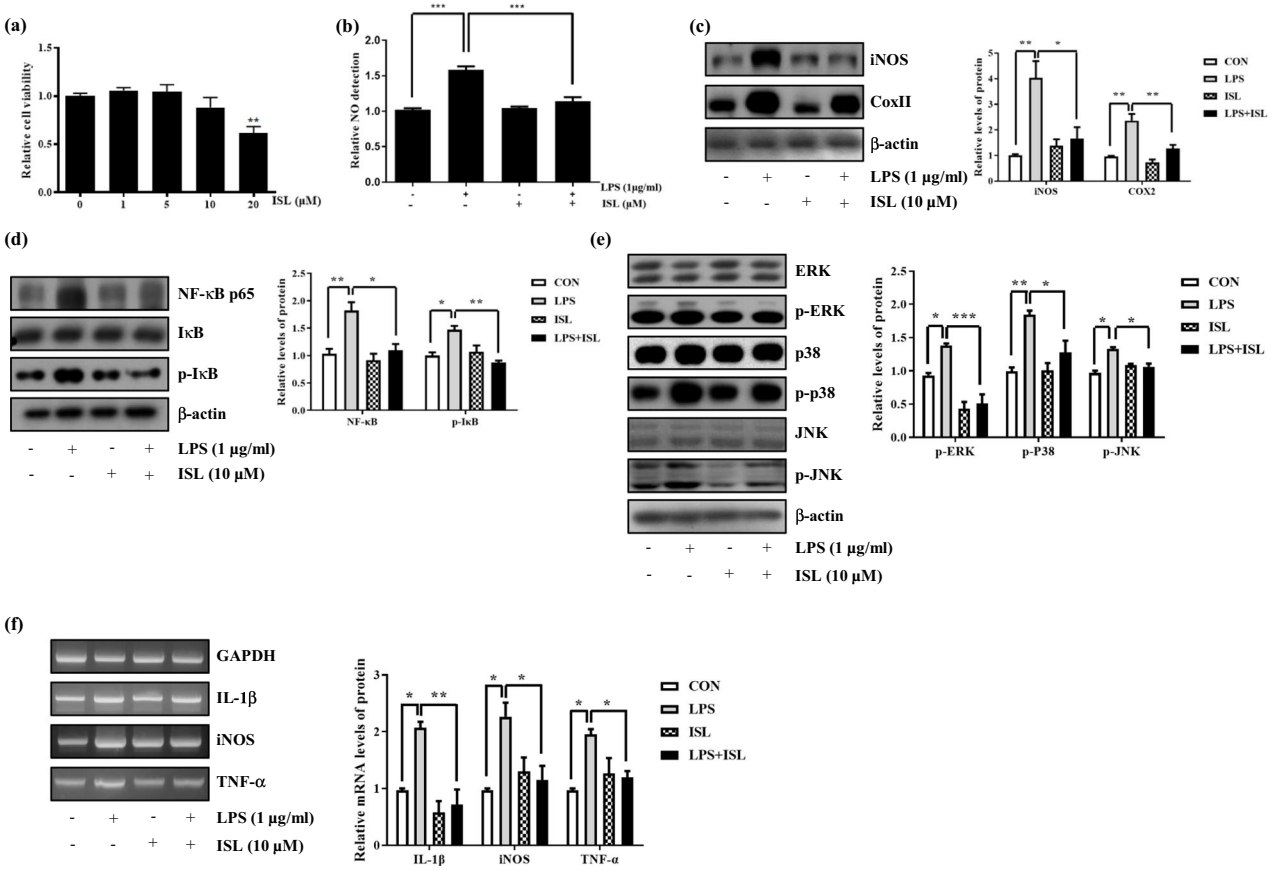

Fig. 1. ISL effects on LPS-induced inflammation. **a** Relative cell viability in BV-2 cells cultured under ISL concentrations (1–20 μM) during 24 h. **b** Relative NO production in 1 μg/mL LPS-treated BV-2 cells with or without ISL for 24 h. **c** Expression levels of iNOS and Cox II were evaluated by western blot analysis. **d** The expression levels of IκB, phosphorylated IκB (p-IκB), and p65 NF-κB were measured by western blot analysis in LPS-treated BV-2 cells with or without 10 μM ISL. **e** Protein levels of ERK, p-ERK, p38, p-P38, JNK, and p-JNK were confirmed by western blot analysis in LPS-treated BV-2 cells with or without 10 μM ISL. **f** The mRNA expression levels of pro-inflammatory cytokines such as IL-1β, iNOS, and TNF-α were analyzed by RT-PCR in LPS-stimulated BV-2 cells with or without 10 μM ISL. Data are presented as means ± SD ($n = 3$). Significance levels: $*p < 0.05$, $**p < 0.01$, and $***p < 0.001$.

studies have identified that ROS production induces mitochondrial fission, and excessive mitochondrial fission is involved in mitochondrial ROS production in microglia [21, 29]. We investigated the effect of ISL on LPS-induced ROS production and mitochondrial dynamics in BV-2 cells. Our results confirm the levels of intracellular and mitochondrial ROS using CM-H2DCFDA and MitoSOX, respectively, in LPS-stimulated BV-2 cells with or without ISL. Results also show that ISL reduced the levels of intracellular and mitochondrial ROS induced by LPS (Fig. 2a and b). We then examined the effect of ISL on LPS-induced change in mitochondrial dynamics. To observe mitochondrial morphology, we used DsRed2-mito expressing BV-2 cells. Mitochondrial morphology was visibly fragmented by the LPS treatment and ISL prevented the shortening of mitochondria (Fig. 2c). Additionally, the LPS-induced decrease in average mitochondrial length was stabilized by pretreatment with ISL (Fig. 2d). Previous studies have shown that LPS mediates mitochondrial fission *via* the dephosphorylation of Drp1 at Ser637 residue in BV-2 cells [21]. Therefore, we investigated the effect of ISL on LPS-induced change in Drp1 phosphorylation levels. Our results showed that ISL ameliorates decreased phosphorylation level of Drp1 at Ser637 induced by LPS, while the Drp1 phosphorylation level at Ser616 remained unchanged (Fig.

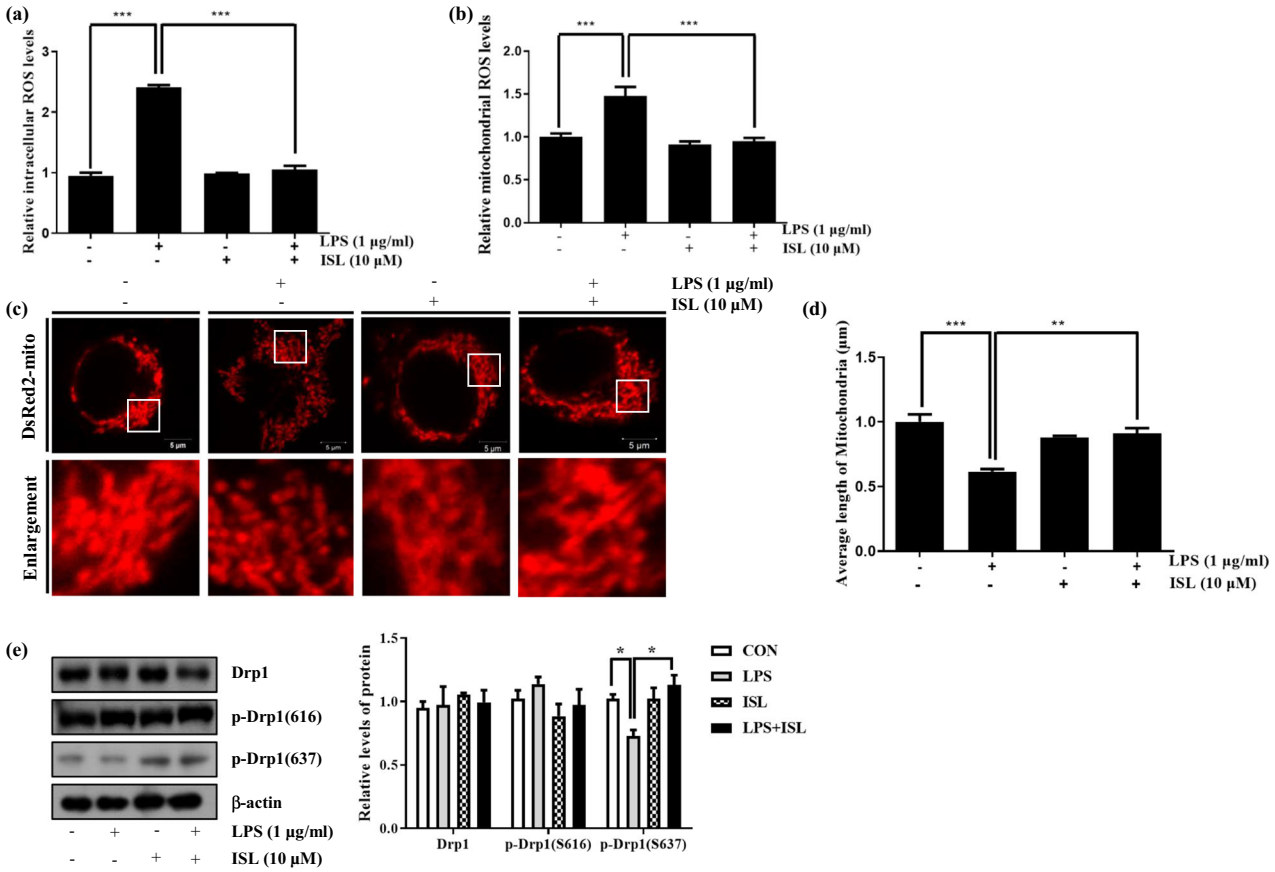

Fig. 2. ISL effects on LPS-induced mitochondrial fission and oxidative stress. Relative intracellular (**a**) and mitochondrial (**b**) ROS levels were assessed using CM-H_2DCFDA and MitoSOX by flow cytometry in LPS-treated BV-2 cells treated with or without 10 μM ISL. (**c**) Mitochondrial morphology was observed by confocal microscopy in LPS-treated DsRed2-mito-expressing BV-2 cells with or without 10 μM ISL. (**d**) Average mitochondrial length was measured by Image J software. (**e**) The expression levels of Drp1, p-Drp1(616), and p-Drp (637) were assessed by western blot analysis in LPS-treated BV-2 cells with or without 10 μM ISL. Data are presented as means ± SD ($n = 3$). Significance levels: $^{*}p < 0.05$, $^{**}p < 0.01$, and $^{***}p < 0.001$.

1e). Our findings suggest that ISL prevents LPS-induced mitochondrial fission *via* dephosphorylation of Drp1 at Ser637 by inhibiting ROS production.

ISL Effect on LPS-Induced Calcium Signaling Pathway

As dephosphorylation of Drp1 at Ser637 is regulated by calcineurin (a calcium-mediated serine/threonine phosphatase) [30], we investigated the effect of ISL on LPS-induced mitochondrial fission relating to the calcium/calcineurin pathways. As shown in Fig. 3a, fluorescence intensity was significantly higher in LPS-induced BV-2 cells, while ISL pretreatment slowed the LPS-induced increase of intracellular calcium (Fig. 3a). Our results also showed that ISL ameliorated LPS-induced calcium levels (Fig. 3b) and it is coincident with in a similar trend as that shown in Fig. 3a. Our examination into the effects of ISL on calcineurin activity in LPS-treated BV-2 cells revealed that cleaved calcineurin levels increased in LPS-induced BV-2 cells compared to the control, while ISL decreased calcineurin levels (Fig. 3c). To confirm these results, we performed an enzyme activity assay in both calcineurin and calpain (a calcineurin upregulator). The results showed that ISL reduced calcineurin and calpain activity in LPS-stimulated BV-2 cells (Fig. 3d and e). These results indicated that LPS causes mitochondrial fission through calcium/calcineurin activation, while ISL inhibited it.

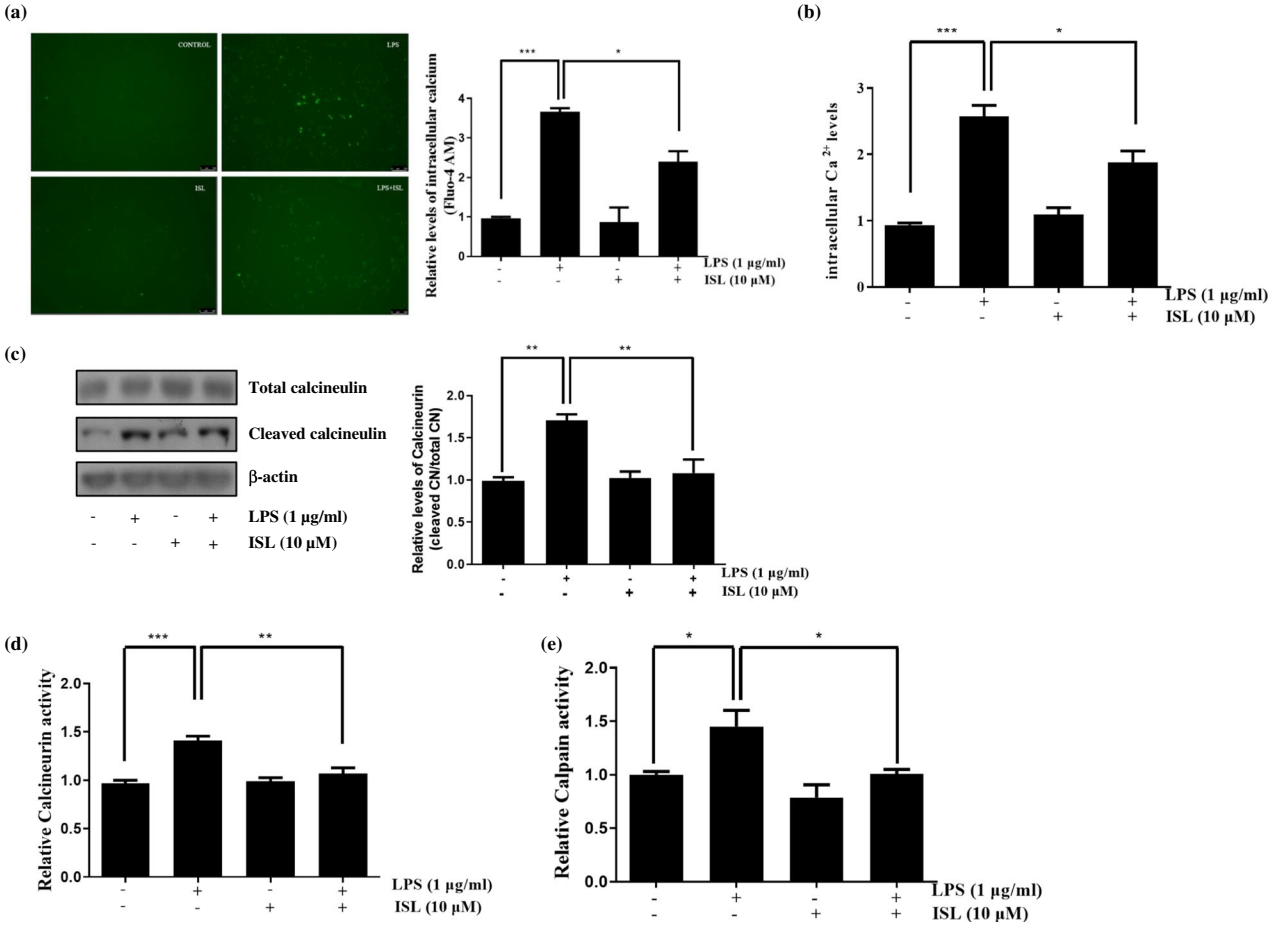

Fig. 3. ISL effect on the LPS-induced calcium signaling pathway. BV-2 cells were incubated with LPS in the presence or absence of 10 μM ISL for 24 h. **a** Intracellular calcium was monitored using Fluo-4 by fluorescence microscopy. Quantification of intracellular calcium was measured using ImageJ software. **b** Intracellular calcium levels were assessed using Fluo-4 by flow cytometry. **c** The expression levels of calcineurin were measured by western blot analysis. The activity of calcineurin **d** and calpain **e** measured using the enzyme activity assay kit. Data are presented as means ± SD ($n = 3$). Significance levels: $^{*}p < 0.05$, $^{**}p < 0.01$, and $^{***}p < 0.001$.

ISL Effect on LPS-Induced Apoptosis

As excessive mitochondrial fission and inflammation are known to cause apoptosis [31, 32], we investigated this effect in LPS-induced BV-2 cells with or without ISL. LPS treatment reduced cell viability, while ISL pretreatment alleviated LPS-induced cell death (Fig. 4a). We also identified apoptosis-related protein factors, such as caspase3, PARP, Bax, and Bcl-2 (Fig. 4b). The levels of Bax, cleaved caspase3, and cleaved PARP were increased by LPS, while the levels of Bcl-2 (an anti-apoptotic factor) were decreased by LPS. ISL pretreatment reduced the concentration of LPS-induced apoptotic factors back to control levels. We further investigated the effect of ISL on LPS-induced apoptosis by flow cytometry with an Annexin V/PI staining. The number of LPS-treated cells during late apoptosis (UR) was significantly higher than the control, while ISL pretreatment alleviated it (Fig. 4c). These results indicated that ISL inhibited the progression of apoptosis induced by LPS in BV-2 cells.

DISCUSSION

Microglial activation regulation plays an important role in the maintenance of neuronal function. The production of abnormal pro-inflammatory factors in activated

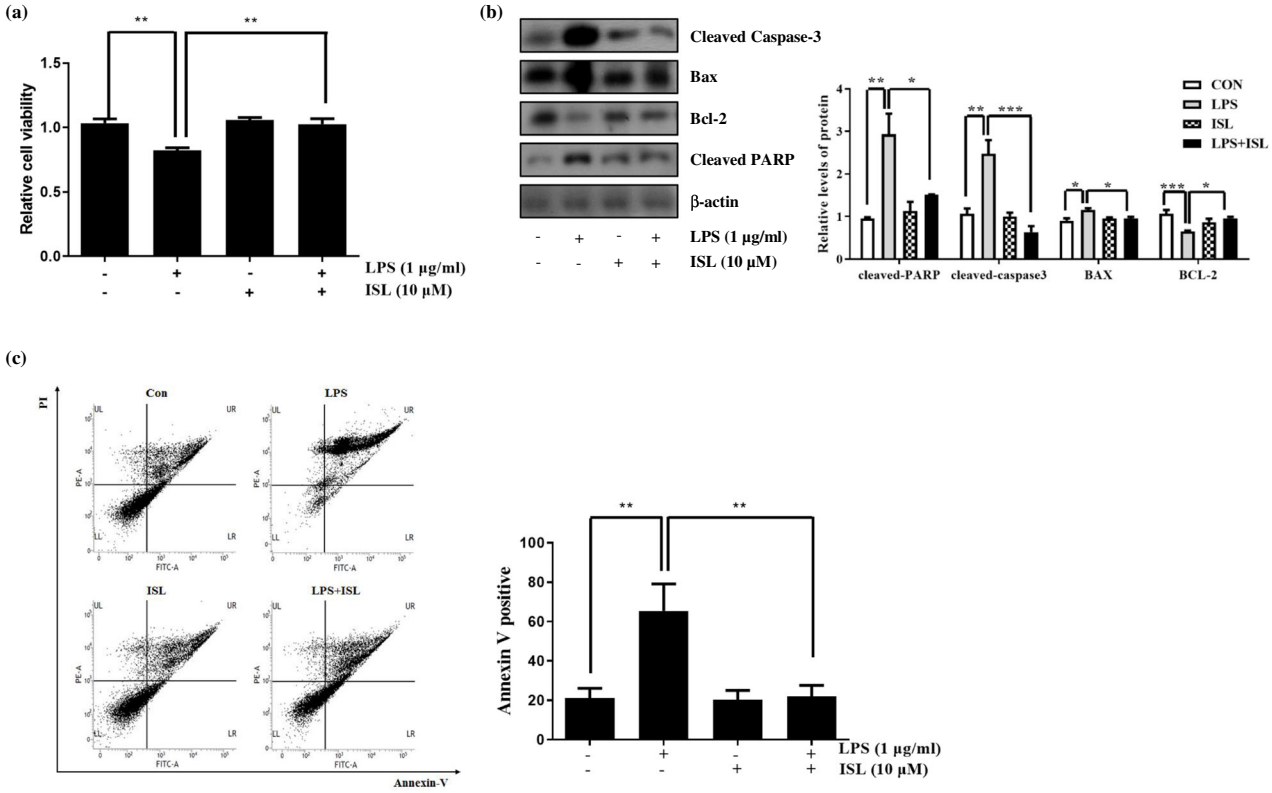

Fig. 4. ISL effect on LPS-induced cell death. BV-2 cells were incubated with LPS in the presence or absence of 10 μM ISL for 24 h. **a** Cell viability was measured by the MTT assay. **b** The protein levels of cleaved caspase3, Bax, Bcl-2, and PARP were evaluated by western blot analysis. **c** Relative levels of cell apoptosis were assessed using Annexin V/PI staining by flow cytometry. The LL quadrant (Annexin-V−/PI−), LR quadrant (Annexin V+/PI−), and UR quadrant (Annexin V+/PI+) indicate the percentage of normal cells, early apoptosis, and late apoptosis, respectively. The graph on the right panel indicated the percentage of late apoptotic cells (UR quadrant). Data are presented as means ± SD ($n = 3$). Statistical significance: $^{*}p < 0.05$, $^{**}p < 0.01$, and $^{***}p < 0.001$.

microglial cells is an important factor leading to the development of neurodegenerative disorders, such as Alzheimer's and Parkinson's disease [33]. The interaction of microglia with other neuroglia affects neurological diseases [33, 34]. In addition, several studies have suggested that abnormal mitochondrial dynamics are associated with a variety of neurodegenerative diseases and neuroinflammation [35–37]; for instance, excessive mitochondrial fission is thought to be involved in microglial activation [37]. There is evidence that isoliquiritigenin (ISL), a compound found in *Glycyrrhizae radix*, has anti-immunomodulatory, anti-oxidative, and antimicrobial effects [22, 38, 39]. More specifically, ISL's anti-inflammatory properties are known to inhibit lipopolysaccharide (LPS)-induced inflammation [22, 39, 40]. Moreover, ISL was found to mitigate mitochondrial fission in glutamate-induced neuronal cells by inhibiting ROS [22]. Therefore, we investigated the mechanism of ISL on LPS-induced inflammatory response and mitochondrial fission in BV-2 cells.

First, we determined the concentration of ISL for our experiment by referring to other studies. The various concentration of ISL is known for its anti-cancer effect. Previous studies have reported successful anti-cancer effects at 5–100 μM ISL in endometrial cancer [7] and 3–10 μM ISL in lung cancer [41]. Furthermore, 10 μM ISL also reduced inflammation by inhibiting NLRP3 inflammation in adipocytes [42], and LPS-induced inflammation was reduced by 10 μM ISL in RAW264.7 macrophages [43]. In another study, an ISL dose of 20 mg/kg was used to alleviate against the damage of blood-brain barrier after traumatic brain injury [44]. In this study, we measured cell viability after ISL treatment at different concentrations. As shown in Fig. 1a, ISL caused apoptosis at > 20 μM;

hence, we used 10 μM ISL for the subsequent experiments. We also showed that ISL alleviated the increase of pro-inflammatory factors (*e.g.*, NO production, MAPK activation, and pro-inflammatory cytokines; Fig. 1b–f), suggesting that 10 μM ISL effectively decreased the pro-inflammatory response induced by LPS in BV-2 cells.

ROS are a well-known factor causing apoptosis or mitochondrial fission in microglia [21, 37, 45]. ROS are also strongly correlated with microglial activation through the MAPK and NF-kB pathways [16, 21, 46, 47]. On the other hand, ISL is known to have a protective effect against neuronal damage by decreasing oxidative stress [6, 24]. As shown in Fig. 2a and b, ISL decreased both intracellular and mitochondrial ROS induced by LPS in BV-2 cells, indicating that ISL's anti-inflammatory effect is related to its antioxidant capacity. In recent experiments, mitochondrial dynamics have been shown to be associated with cellular functions and ROS regulation [48]. Drp1, an important factor in mitochondrial fission, is known to be activated by the phosphorylation of serine 616 and the dephosphorylation of serine 637 [30]. Previous study has been identified that LPS-induced microglial activation causes mitochondrial fission through the dephosphorylation of Drp1 at serine 637 residues [21]. As shown in Fig. 2c–e, LPS-induced mitochondrial fission *via* the dephosphorylation of Drp1 at serine 637 was reduced by ISL as it inhibited ROS production.

Drp1 serine 637 residues are known to be phosphorylated by PKA and dephosphorylated by calcineurin [30]. Calcineurin is a serine/threonine phosphatase, activated through calcium/calmodulin-dependent or calcium/calmodulin-independent activation [49, 50]. The increase in calcium caused by LPS is closely related to microglial activation [51]. Thus, we hypothesized that ISL inhibits the calcium/calcineurin pathway induced by LPS and mitigate mitochondrial fission. Therefore, we investigated the effect of ISL on intracellular calcium changes induced by LPS. ISL inhibited the increase in calcium levels induced by LPS in BV-2 cells (Fig. 3a and b) and effectively reduced LPS-induced activation of calcineurin and calpain (Fig. 3c–e), indicating that ISL reduced LPS-induced mitochondrial fission by inhibiting the calcium/calcineurin pathway, and consequently alleviates the pro-inflammatory response. However, the precise mechanism pathway explaining the relationship between ISL' s antioxidant effect and calcium inhibition requires further research.

We also examined the effect of ISL on LPS-induced microglial apoptosis. The inflammatory response of microglial activation is also closely associated with apoptosis [3]. A previous study has shown that microglial cells in LPS- and INF-γ-exposed mice underwent apoptosis [52]. Moreover, treatment with 1 ng/mL of LPS activated TNF-α and caspase-3 in microglial cells [3]. As shown in Fig. 4, LPS induced apoptosis and increased apoptotic factors, which were then attenuated by ISL, suggesting that ISL reduces the inflammatory response by inhibiting mitochondrial fission and consequently reducing microglial apoptosis.

Our results demonstrate for the first time that ISL has a protective effect against LPS-induced inflammatory response through the inhibition of mitochondrial fission. Overall, our findings suggest that ISL significantly reduced mitochondrial fission, inflammation, and microglial apoptosis by inhibiting ROS and calcium/calcineurin pathway in LPS-stimulated microglial cells (Supplementary Fig. 1). These findings suggest that ISL can play an important role in the prevention of neuroinflammation and may provide new treatment modalities for neuroinflammation-mediated disorders. However, further research is required to investigate the exact mechanism through which ISL induces anti-inflammatory effects and calcium inhibition.

FUNDING

This research was supported by the National Research Foundation of Korea (NRF) grant funded by the Korea government (NRF-2020R1A2B5B01002563 and MSIT, NRF-2017R1A5A2015391) and the KRIBB Research Initiative Program (KGM4622013).

COMPLIANCE WITH ETHICAL STANDARDS

Conflict of Interest. The authors declare that they have no conflict of interest.

REFERENCES

1. Yang, I., S.J. Han, G. Kaur, C. Crane, and A.T. Parsa. 2010. The role of microglia in central nervous system immunity and glioma immunology. *Journal of Clinical Neuroscience* 17: 6–10.
2. Streit, W.J., J.R. Conde, S.E. Fendrick, B.E. Flanary, and C.L. Mariani. 2005. Role of microglia in the central nervous system's immune response. *Neurological Research* 27: 685–691.

3. Liu, B., K. Wang, H.M. Gao, B. Mandavilli, J.Y. Wang, and J.S. Hong. 2001. Molecular consequences of activated microglia in the brain: overactivation induces apoptosis. *Journal of Neurochemistry* 77: 182–189.
4. Mrak, R.E. 2012. Microglia in Alzheimer brain: a neuropathological perspective. *International Journal of Alzheimer's Disease* 2012: 165021.
5. Imamura, K., M. Sawada, N. Ozaki, H. Naito, N. Iwata, R. Ishihara, T. Takeuchi, and H. Shibayama. 2001. Activation mechanism of brain microglia in patients with diffuse neurofibrillary tangles with calcification: a comparison with Alzheimer disease. *Alzheimer Disease and Associated Disorders* 15: 45–50.
6. Zeng, J., Y. Chen, R. Ding, L. Feng, Z. Fu, S. Yang, X. Deng, Z. Xie, and S. Zheng. 2017. Isoliquiritigenin alleviates early brain injury after experimental intracerebral hemorrhage via suppressing ROS- and/or NF-kappaB-mediated NLRP3 inflammasome activation by promoting Nrf2 antioxidant pathway. *Journal of Neuroinflammation* 14: 119.
7. Wu, C.H., H.Y. Chen, C.W. Wang, T.M. Shieh, T.C. Huang, L.C. Lin, K.L. Wang, and S.M. Hsia. 2016. Isoliquiritigenin induces apoptosis and autophagy and inhibits endometrial cancer growth in mice. *Oncotarget* 7: 73432–73447.
8. Patricia Moreno-Londono, A., C. Bello-Alvarez, and J. Pedraza-Chaverri. 2017. Isoliquiritigenin pretreatment attenuates cisplatin induced proximal tubular cells (LLC-PK1) death and enhances the toxicity induced by this drug in bladder cancer T24 cell line. *Food and Chemical Toxicology* 109: 143–154.
9. Kim, J.Y., S.J. Park, K.J. Yun, Y.W. Cho, H.J. Park, and K.T. Lee. 2008. Isoliquiritigenin isolated from the roots of Glycyrrhiza uralensis inhibits LPS-induced iNOS and COX-2 expression via the attenuation of NF-kappaB in RAW 264.7 macrophages. *European Journal of Pharmacology* 584: 175–184.
10. Szabadkai, G., A.M. Simoni, K. Bianchi, D. De Stefani, S. Leo, M.R. Wieckowski, et al. 1763. Mitochondrial dynamics and Ca2+ signaling. *Biochimica et Biophysica Acta* 2006: 442–449.
11. Bertero, E., and C. Maack. 2018. Calcium signaling and reactive oxygen species in mitochondria. *Circulation Research* 122: 1460–1478.
12. Murphy, M.P. 2013. Mitochondrial dysfunction indirectly elevates ROS production by the endoplasmic reticulum. *Cell Metabolism* 18: 145–146.
13. Newsholme, P., V.F. Cruzat, K.N. Keane, R. Carlessi, and P.I. de Bittencourt Jr. 2016. Molecular mechanisms of ROS production and oxidative stress in diabetes. *The Biochemical Journal* 473: 4527–4550.
14. Ding, X., M. Zhang, R. Gu, G. Xu, and H. Wu. 2017. Activated microglia induce the production of reactive oxygen species and promote apoptosis of co-cultured retinal microvascular pericytes. *Graefe's Archive for Clinical and Experimental Ophthalmology* 255: 777–788.
15. Kim, E.K., and E.J. Choi. 1802. Pathological roles of MAPK signaling pathways in human diseases. *Biochimica et Biophysica Acta* 2010: 396–405.
16. Park, J., J.S. Min, B. Kim, U.B. Chae, J.W. Yun, M.S. Choi, I.K. Kong, K.T. Chang, and D.S. Lee. 2015. Mitochondrial ROS govern the LPS-induced pro-inflammatory response in microglia cells by regulating MAPK and NF-kappaB pathways. *Neuroscience Letters* 584: 191–196.
17. Kasahara, E., A. Sekiyama, M. Hori, K. Hara, N. Takahashi, M. Konishi, E.F. Sato, S. Matsumoto, H. Okamura, and M. Inoue. 2011. Mitochondrial density contributes to the immune response of macrophages to lipopolysaccharide via the MAPK pathway. *FEBS Letters* 585: 2263–2268.
18. Westermann, B. 2010. Mitochondrial fusion and fission in cell life and death. *Nature Reviews. Molecular Cell Biology* 11: 872–884.
19. Wang, X., B. Su, H.G. Lee, X. Li, G. Perry, M.A. Smith, and X. Zhu. 2009. Impaired balance of mitochondrial fission and fusion in Alzheimer's disease. *The Journal of Neuroscience* 29: 9090–9103.
20. Knott, A.B., G. Perkins, R. Schwarzenbacher, and E. Bossy-Wetzel. 2008. Mitochondrial fragmentation in neurodegeneration. *Nature Reviews. Neuroscience* 9: 505–518.
21. Park, J., H. Choi, J.S. Min, S.J. Park, J.H. Kim, H.J. Park, B. Kim, J.I. Chae, M. Yim, and D.S. Lee. 2013. Mitochondrial dynamics modulate the expression of pro-inflammatory mediators in microglial cells. *Journal of Neurochemistry* 127: 221–232.
22. Lee, D.G., J.S. Min, H.S. Lee, and D.S. Lee. 2018. Isoliquiritigenin attenuates glutamate-induced mitochondrial fission via calcineurin-mediated Drp1 dephosphorylation in HT22 hippocampal neuron cells. *Neurotoxicology* 68: 133–141.
23. Zhang, X., P. Zhu, X. Zhang, Y. Ma, W. Li, J.M. Chen, et al. 2013. Natural antioxidant-isoliquiritigenin ameliorates contractile dysfunction of hypoxic cardiomyocytes via AMPK signaling pathway. *Mediators of Inflammation* 2013: 390890.
24. Yang, E.J., J.S. Min, H.Y. Ku, H.S. Choi, M.K. Park, M.K. Kim, K.S. Song, and D.S. Lee. 2012. Isoliquiritigenin isolated from Glycyrrhiza uralensis protects neuronal cells against glutamate-induced mitochondrial dysfunction. *Biochemical and Biophysical Research Communications* 421: 658–664.
25. Vijitruth, R., M. Liu, D.Y. Choi, X.V. Nguyen, R.L. Hunter, and G. Bing. 2006. Cyclooxygenase-2 mediates microglial activation and secondary dopaminergic cell death in the mouse MPTP model of Parkinson's disease. *Journal of Neuroinflammation* 3: 6.
26. Sierra, A., J. Navascues, M.A. Cuadros, R. Calvente, D. Martin-Oliva, R.M. Ferrer-Martin, et al. 2014. Expression of inducible nitric oxide synthase (iNOS) in microglia of the developing quail retina. *PLoS One* 9: e106048.
27. Kaminska, B., A. Gozdz, M. Zawadzka, A. Ellert-Miklaszewska, and M. Lipko. 2009. MAPK signal transduction underlying brain inflammation and gliosis as therapeutic target. *Anat Rec (Hoboken)* 292: 1902–1913.
28. Bachstetter, A.D., B. Xing, L. de Almeida, E.R. Dimayuga, D.M. Watterson, and L.J. Van Eldik. 2011. Microglial p38alpha MAPK is a key regulator of proinflammatory cytokine up-regulation induced by toll-like receptor (TLR) ligands or beta-amyloid (Abeta). *Journal of Neuroinflammation* 8: 79.
29. Distelmaier, F., F. Valsecchi, M. Forkink, S. van Emst-de Vries, H.G. Swarts, R.J. Rodenburg, et al. 2012. Trolox-sensitive reactive oxygen species regulate mitochondrial morphology, oxidative phosphorylation and cytosolic calcium handling in healthy cells. *Antioxidants & Redox Signaling* 17: 1657–1669.
30. Cereghetti, G.M., A. Stangherlin, O. Martins de Brito, C.R. Chang, C. Blackstone, P. Bernardi, et al. 2008. Dephosphorylation by calcineurin regulates translocation of Drp1 to mitochondria. *Proceedings of the National Academy of Sciences of the United States of America* 105: 15803–15808.
31. Youle, R.J., and M. Karbowski. 2005. Mitochondrial fission in apoptosis. *Nature Reviews. Molecular Cell Biology* 6: 657–663.
32. Bossy-Wetzel, E., M.J. Barsoum, A. Godzik, R. Schwarzenbacher, and S.A. Lipton. 2003. Mitochondrial fission in apoptosis, neurodegeneration and aging. *Current Opinion in Cell Biology* 15: 706–716.
33. Dheen, S.T., C. Kaur, and E.A. Ling. 2007. Microglial activation and its implications in the brain diseases. *Current Medicinal Chemistry* 14: 1189–1197.
34. Kaminsky, N., O. Bihari, S. Kanner, and A. Barzilai. 2016. Connecting malfunctioning glial cells and brain degenerative disorders. *Genomics, Proteomics & Bioinformatics* 14: 155–165.

35. Bertholet, A.M., T. Delerue, A.M. Millet, M.F. Moulis, C. David, M. Daloyau, L. Arnauné-Pelloquin, N. Davezac, V. Mils, M.C. Miquel, M. Rojo, and P. Belenguer. 2016. Mitochondrial fusion/fission dynamics in neurodegeneration and neuronal plasticity. *Neurobiology of Disease* 90: 3–19.
36. Lu, B. 2009. Mitochondrial dynamics and neurodegeneration. *Current Neurology and Neuroscience Reports* 9: 212–219.
37. Katoh, M., B. Wu, H.B. Nguyen, T.Q. Thai, R. Yamasaki, H. Lu, et al. 2017. Polymorphic regulation of mitochondrial fission and fusion modifies phenotypes of microglia in neuroinflammation. *Scientific Reports* 7: 4942.
38. Link, P., and M. Wink. 2019. Isoliquiritigenin exerts antioxidant activity in Caenorhabditis elegans via insulin-like signaling pathway and SKN-1. *Phytomedicine* 55: 119–124.
39. Peng, F., Q. Du, C. Peng, N. Wang, H. Tang, X. Xie, et al. 2015. A review: the pharmacology of Isoliquiritigenin. *Phytotherapy Research* 29: 969–977.
40. Zhou, J.X., and Wink, M. 2019. Evidence for anti-Inflammatory activity of isoliquiritigenin, 18beta glycyrrhetinic acid, ursolic acid, and the traditional Chinese medicine plants Glycyrrhiza glabra and Eriobotrya japonica, at the molecular level. *Medicines (Basel)* 6(2): 5.
41. Chen, C., A.K. Shenoy, R. Padia, D. Fang, Q. Jing, P. Yang, S.B. Su, and S. Huang. 2018. Suppression of lung cancer progression by isoliquiritigenin through its metabolite 2, 4, 2′, 4'-Tetrahydroxychalcone. *Journal of Experimental & Clinical Cancer Research* 37: 243.
42. Honda, H., Y. Nagai, T. Matsunaga, N. Okamoto, Y. Watanabe, K. Tsuneyama, H. Hayashi, I. Fujii, M. Ikutani, Y. Hirai, A. Muraguchi, and K. Takatsu. 2014. Isoliquiritigenin is a potent inhibitor of NLRP3 inflammasome activation and diet-induced adipose tissue inflammation. *Journal of Leukocyte Biology* 96: 1087–1100.
43. Lee, S.H., J.Y. Kim, G.S. Seo, Y.C. Kim, and D.H. Sohn. 2009. Isoliquiritigenin, from Dalbergia odorifera, up-regulates anti-inflammatory heme oxygenase-1 expression in RAW264.7 macrophages. *Inflammation Research* 58: 257–262.
44. Zhang, M., Y. Wu, L. Xie, C.H. Teng, F.F. Wu, K.B. Xu, X. Chen, J. Xiao, H.Y. Zhang, and D.Q. Chen. 2019. Corrigendum to "Isoliquiritigenin protects against blood-brain barrier damage and inhibits the secretion of pro-inflammatory cytokines in mice after traumatic brain injury" [International Immunopharmacology 65(2018) 64–75]. *International Immunopharmacology* 67: 490.
45. Ge, J., C. Wang, X. Nie, J. Yang, H. Lu, X. Song, K. Su, T. Li, J. Han, Y. Zhang, J. Mao, Y. Gu, J. Zhao, S. Jiang, and Q. Wu. 2016. ROS-mediated apoptosis of HAPI microglia through p53 signaling following PFOS exposure. *Environmental Toxicology and Pharmacology* 46: 9–16.
46. Pawate, S., Q. Shen, F. Fan, and N.R. Bhat. 2004. Redox regulation of glial inflammatory response to lipopolysaccharide and interferon gamma. *Journal of Neuroscience Research* 77: 540–551.
47. Torres, M. 2003. Mitogen-activated protein kinase pathways in redox signaling. *Frontiers in Bioscience* 8: d369–d391.
48. Jezek, J., Cooper, K.F., and Strich, R. 2018. Reactive oxygen species and mitochondrial dynamics: the Yin and Yang of mitochondrial dysfunction and cancer progression. *Antioxidants (Basel)* 7(1): 13.
49. Onodera, H., Y. Yamasaki, K. Kogure, and E. Miyamoto. 1995. Calcium/calmodulin-dependent protein kinase II and protein phosphatase 2B (calcineurin) immunoreactivity in the rat hippocampus long after ischemia. *Brain Research* 684: 95–98.
50. Bandyopadhyay, J., J. Lee, J. Lee, J.I. Lee, J.R. Yu, C. Jee, J.H. Cho, S. Jung, M.H. Lee, S. Zannoni, A. Singson, D.H. Kim, H.S. Koo, and J. Ahnn. 2002. Calcineurin, a calcium/calmodulin-dependent protein phosphatase, is involved in movement, fertility, egg laying, and growth in Caenorhabditis elegans. *Molecular Biology of the Cell* 13: 3281–3293.
51. Tvrdik, P., and Kalani, M.Y.S. 2017. In vivo imaging of microglial calcium signaling in brain inflammation and injury. *Int J Mol Sci* 18(11): 2366.
52. Lee, P., J. Lee, S. Kim, M.S. Lee, H. Yagita, S.Y. Kim, H. Kim, and K. Suk. 2001. NO as an autocrine mediator in the apoptosis of activated microglial cells: correlation between activation and apoptosis of microglial cells. *Brain Research* 892: 380–385.